Geophysical Journal International

Geophys. J. Int. (2022) **231,** 1404–1420
Advance Access publication 2022 June 29
GJI Gravity, Geodesy and Tides

https://doi.org/10.1093/gji/ggac249

Moho depths for Antarctica Region by the inversion of ground-based gravity data

Alessandra Borghi

INGV - sezione di Bologna, Via Donato Creti 12, 40100 *Bologna. E-mail: alessandra.borghi@ingv.it*

Accepted 2022 June 23. Received 2022 June 23; in original form 2022 April 13

SUMMARY

In the last years the scientific literature has been enriched with new models of the Moho depth in the Antarctica Continent derived by the seismic reflection technique and refraction profiles, receiver functions and seismic surface waves, but also by gravimetric observations over the continent. In particular, the gravity satellite missions of the last two decades have provided data in this remote region of the Earth and have allowed the investigation of the crust properties. Meanwhile, other important contributions in this direction has been given by the fourth International Polar Year (IPY, 2007–2008) which started seismographic and geodetic networks of unprecedented duration and scale, including airborne gravimetry over largely unexplored Antarctic frontiers. In this study, a new model for the Antarctica Moho depths is proposed. This new estimation is based on no satellite gravity measures, thanks to the availability of the gravity database ANTGG2015, that collects gravity data from ground-base, airborne and shipborne campaigns. In this new estimate of the Moho depths the contribution of the gravity measures has been maximized reducing any correction of the gravity measures and avoiding constraints of the solution to seismological observations and to geological evidence. With this approach a pure gravimetric solution has been determined. The model obtained is pretty in agreement with other Moho models and thanks to the use of independent data it can be exploited also for cross-validating different Moho depths solutions.

Key words: Antarctica; Moho; Gravity inversion; Collocation; ANTGG2015.

1 INTRODUCTION

In the last years different methods for the definition of Moho depth were presented and tested, based on gravimetric data and possibly integrated with Moho depths derived by seismic observations. One of the most used methods is essentially based on the forward approach in the so called Parker–Oldenburg method, based on theoretic works of Vening Meinesz (1931), Bott (1960) and Parker (1973) that provided a rapid calculation of the gravitational anomaly caused by a 2-D uneven layer of material (Oldenburg 1974). More recently, the Parker–Oldenburg method has been generalized by Gómez-Ortiz & Agarwal (2005) and Shin *et al*. (2007) for 3-D inversion. The Parker–Oldenburg method is based on the forward modelling of the topographic effects in terms of gravity of rectangular prisms and can be fast solved using FFT-technique. In recent years this method has been improved to take the spherical approximation of the Earth into account, because more often the gravity inversion methods involve wide regions of the Earth. Chen & Tenzer (2020) developed Parker–Oldenburg method for Earth's spherical approximation and Uieda & Barbosa (2017) implemented tesseroids, that are spherical prisms, to compute the gravity effects of the topography, taking into account for the curvature of the Earth's surface.

Tenzer *et al*. (2009) improved the CRUST2.0 model (Bassin *et al*. 2000) using EGM2008 geopotential model (Pavlis *et al*. 2012) and correcting the gravity disturbances for the gravitational effects of the topography and of the density contrast of oceans, sediments, ice and crust down to the Moho discontinuity. Bagherbandi *et al*. (2013, 2015) and Tenzer *et al*. (2015) determined the Moho depths using a combined seismic–gravimetric model, which combines CRUST1.0 and the modified Vening Meinesz-Moritz method (Moritz 1990), solving the modified Vening Meinesz-Moritz inverse problem of isostasy.

Eshagh *et al*. (2011) propose an inversion method based on the integration of gravity and seismic information according to the isostatic equilibrium principle and performing the combination using spherical harmonic analysis; Reguzzoni *et al*. (2013) combine the seismic global model CRUST2.0 (Bassin *et al*. 2000) with gravity observations from the GOCE satellite mission using spherical harmonic analysis. Rossi

Table 1. Table with the characteristics of some geodetic models of the Antarctica Moho. GGM, global gravity model; S, satellite; full, gravity data from satellite, ground and altimetry.

Reference	Model name	Data	Seismic depth constraints
Pappa *et al*. (2019)	PAP19	S-GGM (GOCO05s)	Yes
Chisenga *et al*. (2019)	CHI19	full-GGM (EIGEN-6C4)	Yes
Block *et al*. (2009)	BLO09	full-GGM (GGM03C)	No
Llubes *et al*. (2018)	LLU18	S-GGM (GO_CONS_GCF_2_DIR_R5)	No
Baranov *et al*. (2018)	BTB18	S-GGM (GOCO05s)	Yes

et al. (2015) and Capponi *et al*. (2022) use a Bayesian probabilistic approach, adjusting both the geometries and the density distribution of the interested volume (discretized in small volumetric elements) in order to fit the gravity data.

Least-square collocation (LSC) theory (Krarup 1969; Tscherning 1985; Moritz 1990) can be also used to solve gravity inversion problems, as the Moho depth estimate. In particular, the contributions of Barzaghi and co-authors is mentioned, that propagate the covariance function of the observed gravity data to the covariance function of the Moho depth (Barzaghi *et al*. 1992), implement the collocation method using as input data the gravity observations and seismic Moho depth values (Barzaghi & Biagi 2014) and applied the Collocation method to global scale for Moho determination, also integrated with local observations (Barzaghi *et al*. 2015). The possibility of introducing lateral and vertical density variations in the least-square collocation scheme was discussed in Reguzzoni *et al*. (2020).

Ebadi *et al*. (2019) tested the coherency of most of these presented gravimetric methods in the estimates of Moho depths of Iran. They concluded that the different inversion gravimetric approaches gave coherent estimates when compared to seismic derived Moho depths.

Gravimetric inversion methods generally suppose a two layers model for the Earth to guarantee the uniqueness of the solution and require the application of a regularization method or the knowledge of an *a priori* target function to reduce the influence of the high frequency errors present in the data. The two layers model can be realized using refined Bouguer gravity anomalies (Hofmann-Wellenhof & Moritz 2006), taking into account for sediments if necessary, whereas the regularization can be performed using, for instance, methods like first-order Tikhonov regularization (Tikhonov & Arsenin 1977) in the derived Parker–Oldenburg methods. Concerning the inversion using LSC, the Collocation is itself a regularization and smoothing method for filtering and predicting values with the use of the covariance function of the observations.

These theoretical studies on the gravimetric inversion methods have been accompanied by the compilation of new global gravity geopotential models (GGM), to which the satellite gravity missions CHAMP, GRACE and GOCE have contributed significantly. Indeed, the last two decades have been characterized by satellite gravity missions, which have improved the knowledge of the Earth gravity field, providing new measures with homogeneous precision and spatial resolution and covering regions where gravimetric ground measurements are lacking for their remoteness. So, new GGMs have been computed, differencing each other for the computation approach and for the data used: which gravity satellite mission data are introduced, satellite-only measures, combined terrestrial, ship-borne data, altimetry and airborne measurements.

The availability of reliable gravimetric data covering the entire Antarctica continent allowed many research groups to estimate the Moho discontinuity surface for this remote continent (Table 1), to improve the spatial resolution in this area, with respect to the global solutions already available (Tenzer *et al*. 2009, 2015; Eshagh *et al*. 2011, 2011; Barzaghi *et al*. 2015; Reguzzoni *et al*. 2013; Reguzzoni & Sampietro 2015; Szwillus *et al*. 2016; Baranov *et al*. 2021).

These gravimetric Moho models for Antarctica differ from each other for the GGM and the inversion method used. Block *et al*. (2009) presented the first gravimetric solutions for the Antarctica Moho, using the GGM03C gravity field model (Tapley *et al*. 2007), derived by altimetry, ground and GRACE data, and applying the Parker–Oldenburg inversion method to estimate the Moho depth. Llubes *et al*. (2018) produced a map of Antarctic crustal thickness computed from the satellite-only GO_CONS_GCF_2_DIR_R5 gravity model (Bruinsma *et al*. 2013) and computed with the Parker–Oldenburg iterative algorithm, using the BEDMAP2 (Fretwell *et al*. 2013) products to reduce the data for the gravity effects of the ice thickness. Pappa *et al*. (2019) inverted the satellite-only GOCO05s gravity values (Mayer-Gürr *et al*. 2015) using the modelling based on the tesseroids (Uieda & Barbosa, 2017), and constrained the model with seismic derived depths. Baranov *et al*. (2018) used the same satellite-only GOCO05s gravity model to obtained a gravimetric Moho depth model and combined this solution with the one obtained interpolating seismic stations and profiles with the Kriging technique, together with BEDMAP2 subglacial bedrock relief. Chisenga *et al*. (2019) inverted the high-order degree global gravity model EIGEN-6C4 (Förste *et al*. 2014), obtained by the combination of altimetry, ground and satellite gravimetric data (GRACE and GOCE) and LAGEOS, using the same inversion method of Uieda & Barbosa (2017). Moreover, Wiens *et al*. (2021) present a model based on an inversion of seismic receiver function and Rayleigh-wave velocities in West Antarctica and central Antarctica, and on GOCE satellite gravity constraints over the entire continent.

Beside the gravimetric models, the Moho surface models derived by seismic data have to be mentioned, because they represent independent solutions with respect to the gravimetric models already presented. In particular, we remember the Baranov and Morelli (2013) model (henceforth called BAR13) that is compiled using seismic data obtained in 1960–2011, through seismic reflection and refraction profiles, receiver functions and surface waves. The model is available in a $1^\circ \times 1^\circ$ resolution grid. An *et al*. (2015) used the Rayleigh wave group velocities retrieved from 122 broad-band seismic stations to produce a 3-D *S*-wave velocity model of the crust, from which a Moho

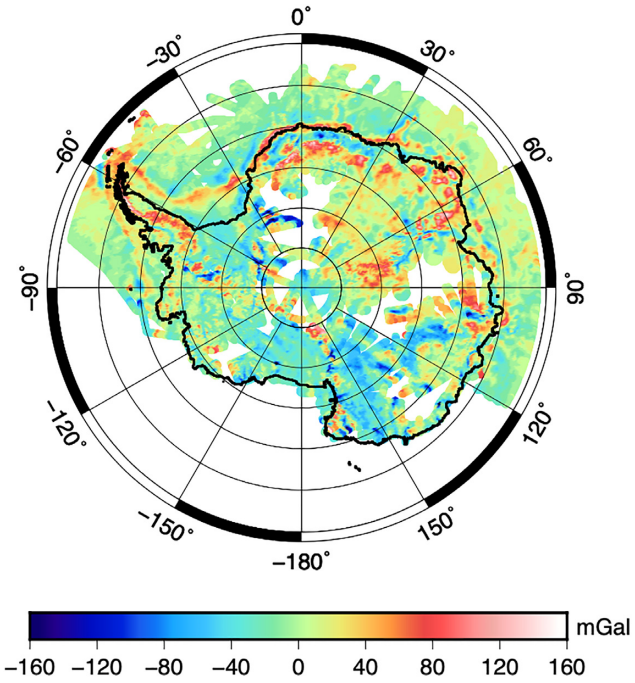

Figure 1. Free-air gravity anomalies in Antarctica from the ANTGG2015 data set (Scheinert *et al*. 2016)

depth map of Antarctica (Moho AN15). Most recent Baranov *et al*. (2021) improve the CRUST1.0 model, using seismic data together with a subglacial bedrock relief from BEDMAP2 database.

All these Moho models, seismic and gravimetric, show a sharp different behaviour between the East and West Antarctica regions: shallower depths characterize West Antarctica with respect to the Eastern Antarctica and with respect to the high depths of the Antarctica Peninsula.

In this work a new estimate of the Moho surface is presented. This new geodetic model is obtained by the ground-based gravity dataset ANTGG2015 (Scheinert *et al*. 2016) and the inversion approach proposed by Barzaghi & Biagi (2014) and Barzaghi *et al*. (2015), based on LSC method. One of the reasons for a new gravimetric estimate of the Moho depths for the Antarctica region was the intention to test the sensitivity of the ANTGG2015 gravity data in the Moho inversion problem, with respect to the inversion of satellite gravity observations and the seismic profiles.

2 METHODS AND DATA PROCESSING

2.1 Gravity data

The ANTGG2015 gravity dataset (Scheinert *et al*. 2016) represents an important collection of validated gravity data for the continent part and some offshore zones of Antarctica, which covers 73 per cent of the continent. The gravity observations come from different ground-base, airborne and shipborne campaigns collected by the geophysical and geodetic communities since the 1980s. The dataset provides a grid of free-air gravity anomalies and of Bouguer anomalies spacing about 10 km (Fig. 1). This important database of ground data does not cover the whole Antarctica Region: some gaps are present in the continental part and the Ross Sea is not covered by observations, however the spatial distribution is enough to try to compute a Moho surface for the entire Antarctica continent.

The free-air gravity anomalies ANTGG2015 have been reduced for the complete Bouguer reduction and isostatic effects according to the Airy-Heiskanen theory (Hofmann Wellenhof & Moritz 2006, Fig. 2). For this purpose, the gravity reduction has been computed using the global Earth2014 Rock Equivalence Topography (RET) (Hirt & Rexer 2015), where the ice and water masses have been substituted with equivalence masses of rock of density 2670 kg m^{-3}. For the Antarctic region the Earth2014 model takes information by Bedmap2 (Fretwell *et al*. 2013). In the Airy-Heiskanen reduction the compensation depth was fixed equal to 30 km and the density of the mantle was 3270 kg m^{-3}. The Earth2014 RET has been also used to estimate the Moho depths predicted by the Airy–Heiskanen theory (Fig. 3). The data has not been reduced for any other gravity signals, as the ones due to sedimentary layers, because the focus of this first estimate of the Antarctica Moho with ground gravity data is the evaluation of the contribution of the gravity information to the definition of this surface, so the use of any other geological or geophysical model, that is CRUST1.0 (Laske *et al*. 2013), has been avoided. In future, the terrain correction reduction could be improved if any well-known density anomalies need to be taken into account. In Table 2 the statistics of the gravity anomalies are reported.

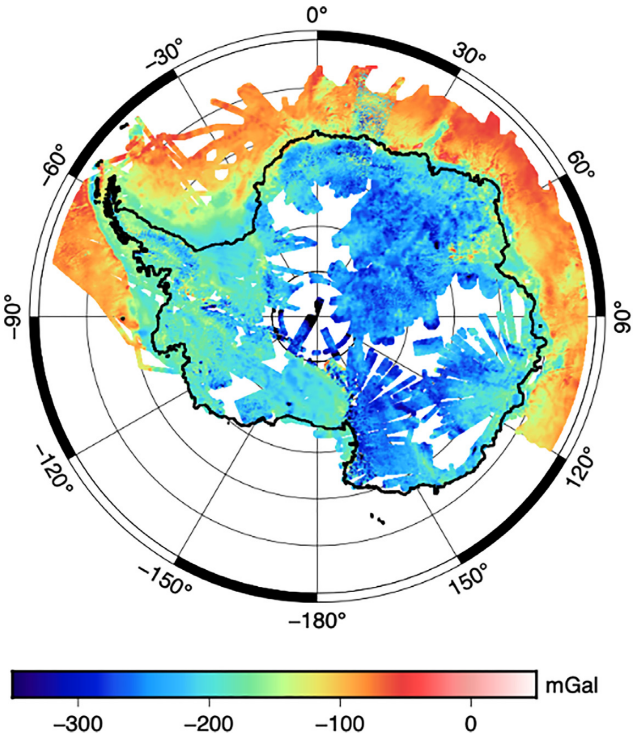

Figure 2. Gravity anomalies in Antarctica from the ANTGG2015 data set (Scheinert *et al*. 2016) reduced for Bouguer anomaly and Airy-Heiskanen isostatic effect.

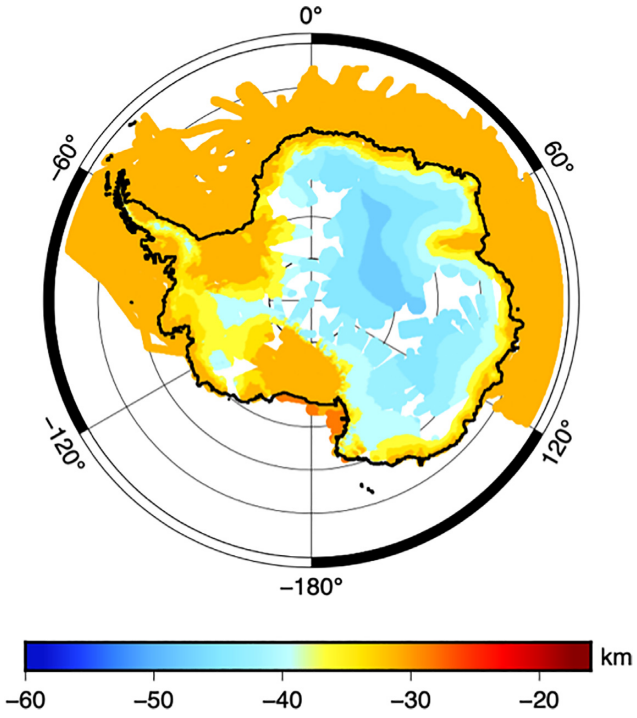

Figure 3. Moho depths predicted by the Airy-Heiskanen isostatic effect using the Earth2014 Rock Equivalence Topography (RET, Hirt & Rexer, 2015)

Table 2. Statistics of the free-air gravity values of the ANTGG2015 database and of the isostatic gravity anomalies. Values in [mGal].

	Mean	*SD*	Min	Max
Δg_{FA}	-0.730	33.054	-384.500	204.800
Δg_{FA} - Δg_{iso}	-180.225	64.527	-565.123	26.126

2.2 Gravity inversion method

In this work it has been chosen to invert the gravity data to estimate the Moho surface using the LSC method, according to the approach proposed by Barzaghi & Biagi (2014) and Barzaghi *et al*. (2015). However, two important changes have been introduced with respect to the method presented in those works and that will be described later: one concerning the reference Moho, that is the separation surface in the two layers model, the other one regarding the collocation estimator.

According to the theoretical approach described in Barzaghi & Biagi (2014), the gravity anomalies are related to the Moho depth by eq. (1), if the gravity is expressed in terms of Cartesian coordinate:

$$\Delta g(x,\ y,\ 0) = G \int\int_{R^2} \mathrm{d}x\ \mathrm{d}y \Delta\rho \frac{\varepsilon \bar{M}}{\left[\bar{M}_0^2 + d_{xy}^2\right]^{3/2}}, \tag{1}$$

where Δg is the gravity anomaly of a two layers configuration; G is the Newton's gravitational constant; $\bar{M}$ is the reference depth of the Moho; ε is the correction with respect to reference depth $\bar{M}$ in a point P, $\Delta\rho$ is the density contrast between the two layers of the model, that is crust and mantle and d_{xy} is the Euclidean distance between the computational point P and the running point Q of the integral over the entire Earth mass. So, in a point P of Cartesian coordinates (x, y) the Moho depth is equal to the sum of the reference Moho $\bar{M}$ plus the correction term ε.

Eq. (1) can be solved using the LSC method to estimate the value of the correction $\varepsilon\,(P)$ with respect to the mean depth $\bar{M}$ in any point P of cartesian coordinate (x, y), as reported in the following equations:

$$\varepsilon\,(P) = \left[C_{\varepsilon\Delta g}^T C_{\varepsilon\varepsilon}^T\right]\ C_{ll}^{-1} l \tag{2}$$

$$l^T = [\Delta g_{\mathrm{obs}} \varepsilon_{\mathrm{obs}}] \tag{3}$$

$$C_{ll} = \left[C_{\Delta g \Delta g_{\mathrm{obs}}} C_{\Delta g \varepsilon}; C_{\varepsilon \Delta g} C_{\varepsilon\varepsilon_{\mathrm{obs}}}\right], \tag{4}$$

where $\boldsymbol{l}$ is the vector of the observations that can be given by the gravity anomalies Δg_{obs} and additionally by some seismic Moho depths $\varepsilon_{\mathrm{obs}}$; $C_{\Delta g_{\mathrm{obs}}}$ is the autocovariance matrix of the gravity anomalies; $C_{\varepsilon\varepsilon_{\mathrm{obs}}}$ is the autocovariance matrix of the Moho depths; $C_{\varepsilon\Delta g}$ is the cross covariance matrix between gravity anomalies and Moho depths.

In this work the Moho surface has been estimated without introducing any information provided by seismic techniques, to have the chance to evaluate the potentiality of the inversion of ANTGG2015 ground gravity database, with respect to the inversion of the gravity satellite observations. For this reason the observation vector is given just by gravity observations and eqs (3) and (4) are simplified are simplified as following:

$$l^T = [\Delta g_{\mathrm{obs}}] \tag{5}$$

$$C_{ll} = \left[C_{\Delta g \Delta g_{\mathrm{obs}}}\right]. \tag{6}$$

In the LSC approach the corrections ε(P) can be estimated using an iterative procedure: after the initial computational step (step-I) its gravity residuals are used for another LSC estimation (step-II), and so on. For any computational point, the total Moho depth is given by the sum of the reference value $\bar{M}$ plus the corrections ε estimated step by step: $\bar{M} + \varepsilon_{\mathrm{I}} + \varepsilon_{\mathrm{II}} + \varepsilon_{\mathrm{III}} \ldots$ The iterative procedure is stopped when the gravity residuals of the LSC start to be uncorrelated values.

At the base of this method there is the sample estimation of the autocovariance function of the gravity anomaly observations $C_{\Delta g \Delta g_{\mathrm{obs}}}$ and the propagation of this autocovariance into the covariance functions of the Moho depths $C_{\varepsilon\varepsilon}$ and into the cross-covariance function $C_{\varepsilon\Delta g}$, as described in Barzaghi and Biagi (2014). The values of the autocovariance matrix can be obtained by the observations through the estimate of the sample autocovariance function (ACF) and fitting the sample values with a positive definite function, to avoid numerical problems in the estimation algorithm, in particular in the inversion of the covariance matrix of the observations (eq. 2). In Cartesian coordinate a possible positive definite function is given by eq. (7), whereas the corresponding cross-covariance function between gravity and the correction to the reference depth of the Moho is reported in eq. (8)

$$C_{\Delta g \Delta g}\ (ax) = \frac{A J_1(ax)}{ax} \tag{7}$$

$$C_{\Delta g \varepsilon}\ (ax) = \frac{1}{2\pi G \Delta\rho}\ \frac{A}{a^2} \int_0^a \mathrm{d}k \cdot kJ\,(kx), \tag{8}$$

where $J_0(.)$ and $J_1(.)$ are the zero and first order Bessel functions, respectively; a and A are the parameters that have to be chosen to fit the sample autocovariance function; x is the distance lag between the computation points (Barzaghi *et al*. 1992).

As it has been introduced in eq. (1), the formulation of the problem requires the definition of an approximated Moho depth $\bar{M}$ and with respect to this reference depth the point-by-point variations ε(P) will be estimated by LSC. In Barzaghi & Biagi (2014) this reference Moho is supposed to be a surface at a constant depth all over the investigated area, however, in a sufficiently wide area, characterized by great variations in the Moho surface depth, a constant mean value is a too restrictive condition. For instance in Barzaghi *et al*. (2015) the authors adopted a

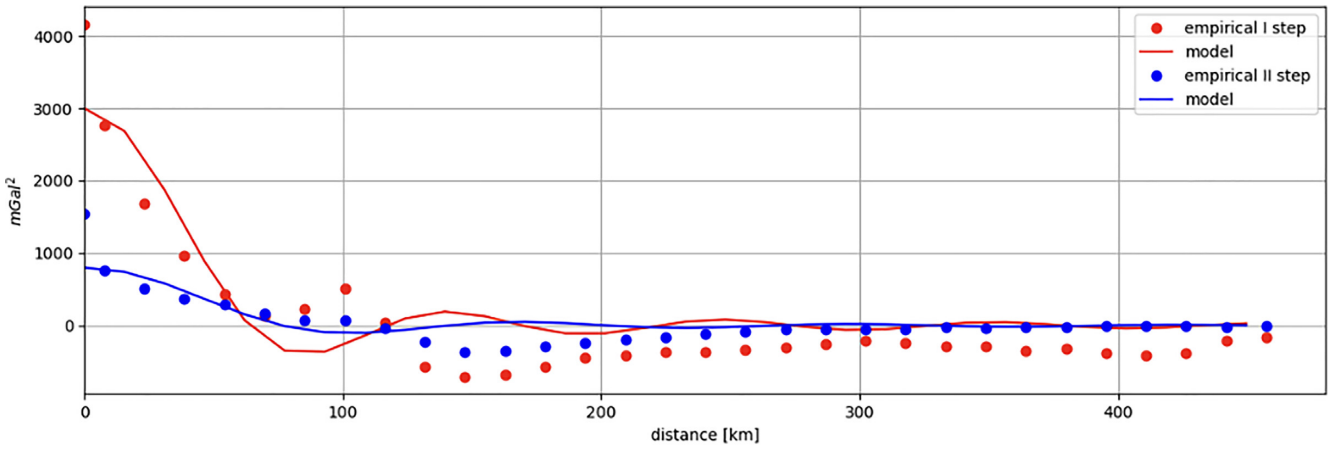

Figure 4. Empirical covariance functions (dots) and their interpolations with positive definite functions (lines) of the Airy–Heiskanen isostatic anomalies (red values) and of the residual of the second iterative step of the LSC computation (blue values)

non constant reference value, computing an approximate global Moho model at first and locally refining the depths by LSC estimation. In this work it has been preferred to use as approximated Moho the surface deducted by Airy–Heiskanen isostatic theory (Hofmann Wellenhof & Moritz 2006), because it is also coherent with the gravity reduction that has been computed to satisfy the two-layers condition. In eq. (9) the classical approach is represented on the left, with respect to the new ones adopted in this work, where $\bar{M}$ can change point by point.

$$\text{standar approach}: M(P) = \bar{M} + \varepsilon(P) \rightarrow \text{new approach}: M(P) = \bar{M}(P) + \varepsilon(P), \tag{9}$$

where M(P) is the Moho at point P, $\bar{M}$ is the constant reference value for the Moho, typically equal to 30 km in the continental area, $\bar{M}(P)$ is the mean value of the Moho that could change point by point P, $\varepsilon(P)$ is the correction with respect to the reference surface, estimated inverting the gravity data with LSC.

The second difference in the methodology used consists in the implementation of a window LSC method (wLSC): given a computation point P, the Moho depth $\varepsilon(P)$ is derived by the gravity observations inside a spherical cap centred in the point P, instead of using all the entire gravity database. The correlation length of the data (about 40 km, Fig. 4) motivates the dimension of the cap. Furthermore, as the method has been developed in planar approximation (Barzaghi *et al.* 1992) because, at regional scale, in a zone ranging $10^\circ \times 10^\circ$ in latitude and longitude, the planar and spherical approximation present differences smaller than 0.5 km (Sampietro 2011). The Antarctica Region extends more than this local approximation, however the wLSC approach, with a window cap significantly smaller than 10°, fixes this problem.

3 RESULTS AND DISCUSSION

3.1 Gravity data inversion

The starting and crucial step in the LSC method is the estimate of the empirical (sample) auto-covariance function (ACF) of the gravity anomalies and its interpolation with a positive definite function as the one of eq. (7).

The sample and model ACFs of the isostatic gravity anomalies computed in this work shows a variance of about 4200 mGal^2 (Fig. 4, red dots and line), coherent with the values reported in Table 2 (standard deviation of about 65 mGal). This variance can be split in the variance of the signal (about 3000 mGal^2) and in the variance of the noise (about 1200 mGal^2), given by the difference between the value in the origin of the x-axis and the second theoretical value. The correlation length of the gravity anomaly is about 40 km and corresponds to the distance between points when the amplitude of the variance of the signal is halved. This short correlation length justifies the use of Cartesian approximation and of the window LSC. The interpolation of the ACF with a positive definite function reported in Fig. 4 is not optimal, however the variance of the signal and the correlation length are well represented by the function used.

For each gravity measurement point the estimate of the correction value $\varepsilon_{\mathrm{I}}(P)$ was computed by LSC inversion of the isostatic gravity anomalies derived from the ANTGG2015 database. The estimated $\varepsilon_{\mathrm{I}}(P)$ values show a clusterization with respect to the position of the computational point P (Fig. 5): for computational points P on land the estimated terms are all positive so this gravity inversion has the effect of lowering the Moho surface in those points; on the sea points the $\varepsilon_{\mathrm{I}}(P)$ values are negative instead and raise the Moho surface toward more common values for ocean plates, reaching around 20 km of depth.

After this first estimate, the residual gravity values obtained by the least-squares collocation estimate were analysed and their ACF has been computed. This second ACF is represented in Fig. 4 using blue dots and the blue line, for the empirical and model functions, respectively. The amplitude of the variance of this residual signal is about one third of the variance of the original isostatic gravity anomalies, both in terms of signal and noise (Table 3). The correlation length is not reduced, so we suppose that it is the effect of the spatial gaps in the database and of other geophysical signals not taken into account in the gravity anomalies reduction, such as the presence of sediment basins. A new least-squares collocation estimate gives the second-step corrections $\varepsilon_{\mathrm{II}}(P)$, that show a quite constant value of about 2 km for the land points

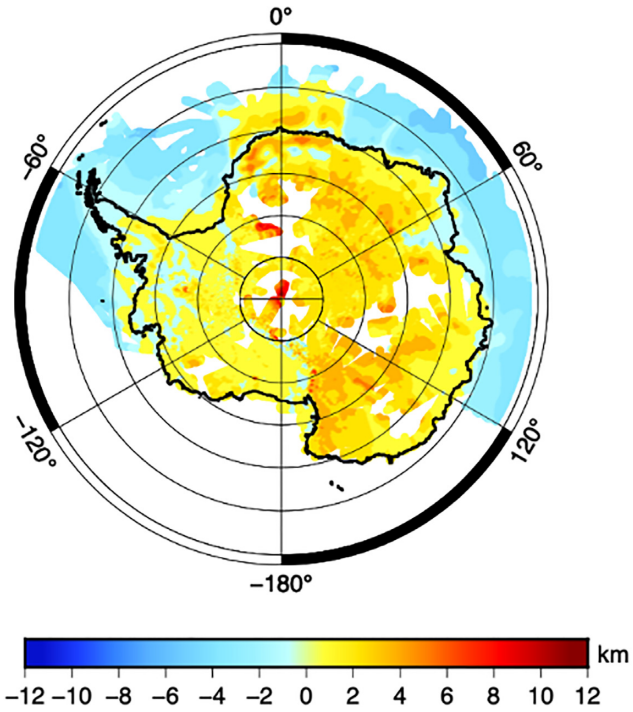

Figure 5. First step corrections (ε_I) to the isostatic Moho surface obtained by the LSC inversion procedure of the ANTGG2015 gravity anomalies.

Table 3. Statistics of the isostatic Moho and of the Moho models estimated with two LSC computations. ε_I and ε_{II} represent the first step and the second step estimates of the LSC procedure, respectively, whereas M_{II} is the total Moho depths (i.e. $M_{II} = M_{iso} + \varepsilon_I + \varepsilon_{II} = M_I + \varepsilon_{II}$). Values in [km].

	Mean	*SD*	Min	Max
M_{iso}	–34.487	5.710	–48.197	–29.734
M_I	–34.189	7.695	–55.378	–24.930
M_{II}	–33.457	7.479	–54.783	–20.105
ε_I	–0.301	2.398	–5.472	10.184
ε_{II}	–0.732	1.228	–7.243	9.501

and more pronunciate corrections for the sea points (Fig. 6). Chisanga *et al*. (2019) and Baranov *et al*. (2018) discussed the presence of important sediment basins mainly offshore and evaluated their effects on the estimate of the Moho depths offshore and onshore, concluding that the gravity effects of the sediments should be removed from the gravity observations before any inversion procedure. However, the choice of the model of sediment for this further correction of the gravity anomalies is not trivial, because the two available models for sediments, Laske & Masters (1997) and Baranov *et al*. (2018), were estimated from sparsely distributed observations and the models differ significantly. For these reasons the data were not reduced for the sediment effects in this new gravity inversion for the Moho. Chisanga *et al*. (2019) affirmed that the effects of thick marine sediment basins can be evaluated in the order of 80 mGal, quantities that can be relevant during the higher steps of the used iterative procedure, so the computation was stopped after the second step of iteration and the final Moho depth model (henceforth called BOR20) has been obtained as the sum $M_{iso} + \varepsilon_I + \varepsilon_{II}$ (Fig. 7).

However, the influence of sediments basins in the estimate of the Moho depths has been tested in a limited zone of Antarctica, the Ronne ice shelf, where Baranov *et al*. (2018, 2021) reported significant layers of sediments that reach up to 14 km in thickness. So, the gravity anomalies have been corrected also for this contribution, using the RET approach and considering the three layers of sediments, and the Moho computation has been repeated for this area, as reported in Section 3.2.

3.2 Discussion

The proposed new gravimetric Moho estimate, BOR20, has been first compared with some of the recent gravimetric Moho models available and listed in Table 1 and with models derived by seismic techniques.

The first check has been carried out with respect to the gravimetric models BLO09, LLU18 and PAP19. These Moho depth surfaces are derived by inverting the gravity data synthesized by GGMs, whereas BOR20 was based on gravity ground measurements. In particular, LLU18 and PAP19 selected GGMs derived by gravity satellite-only missions and also the computation methods are different from the LSC

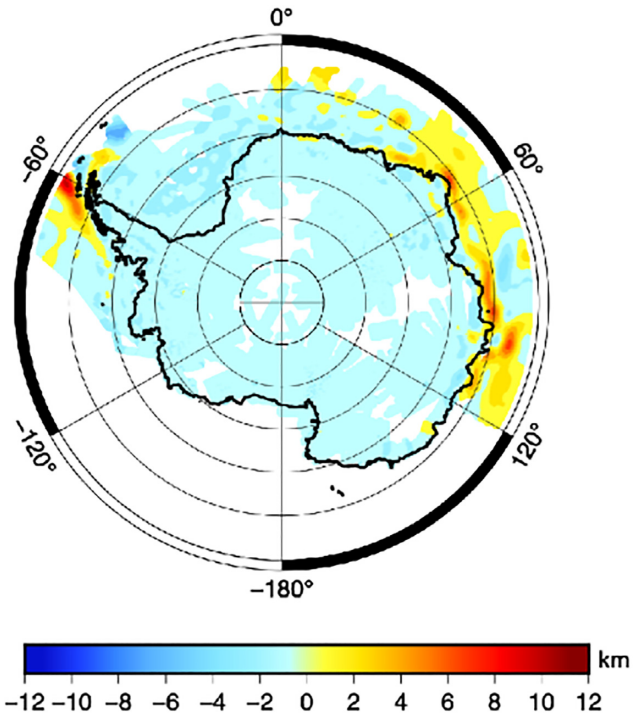

Figure 6. Second step corrections (ε_{II}) to the isostatic Moho surface obtained by the LSC inversion procedure of the ANTGG2015 gravity anomalies.

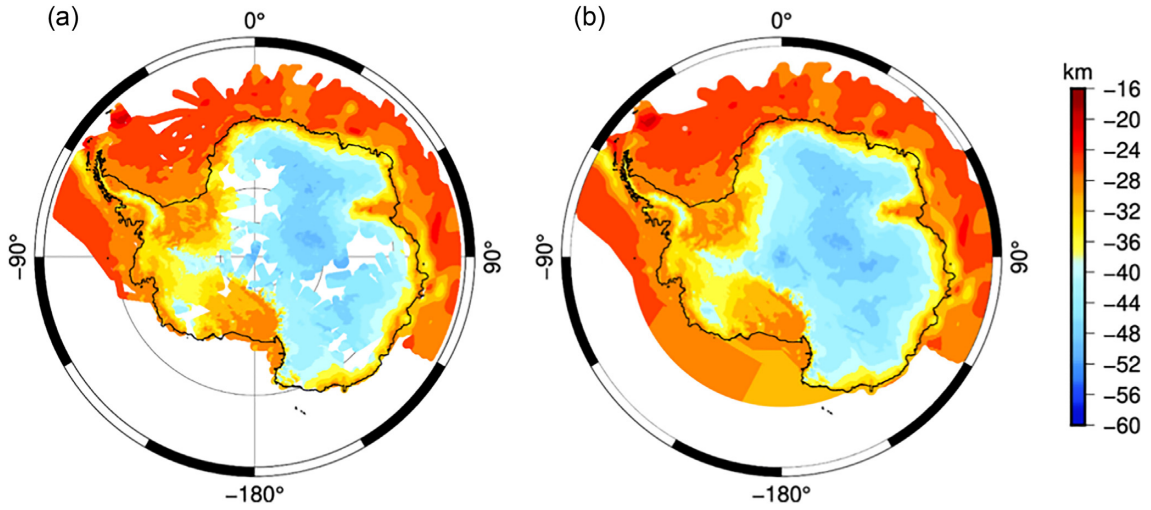

Figure 7. Moho depths of the new gravimetric model BOR20 on the ANTGG2015 gravity points (panel a) and gridded Moho depths BOR20 (panel b), masked in the sea basins where the gravity data are not available.

approach used for the BOR20 estimate. For these reasons BOR20 is quite an independent solution with respect to these later solutions, except for the using of the same topographic and ice models in the gravity data reduction.

In Fig. 8 the differences between the BOR20 depths and the other gravimetric models are reported and some considerations are evident: the PAP19 Moho is systematically shallower than the BOR20 model except along the Transantarctic Mountains (TAM), because we consider the depths as negative values with respect to the sea surface level. BLO09 Moho is very shallow too with respect to the BOR20 model, except for the Ronne Ice Shelf and the Ross Ice Shelf, furthermore BLO09 is a very smooth surface, because the values are in a range of 10 km between –30 to –40 km of depth. With respect to the LLU18 model the BOR20 model is deeper in East Antarctica (EANT) and shallower in West Antarctica (WANT). It means that the difference in the crust thickness between west and east Antarctica is more pronounced in the BOR20 model. Summarizing these results, in EANT the BOR20 model, based on ground-based gravity data, is deeper with respect to the other gravimetric models taken into account, whereas in WANT region BOR20 is shallower in the ice shelves, as Ross and Ronne ice Shelf.

The second type of comparison has been done with respect to the Moho depths deducted by seismic observations and derived by seismic Moho models, as AN15 and BAR13.

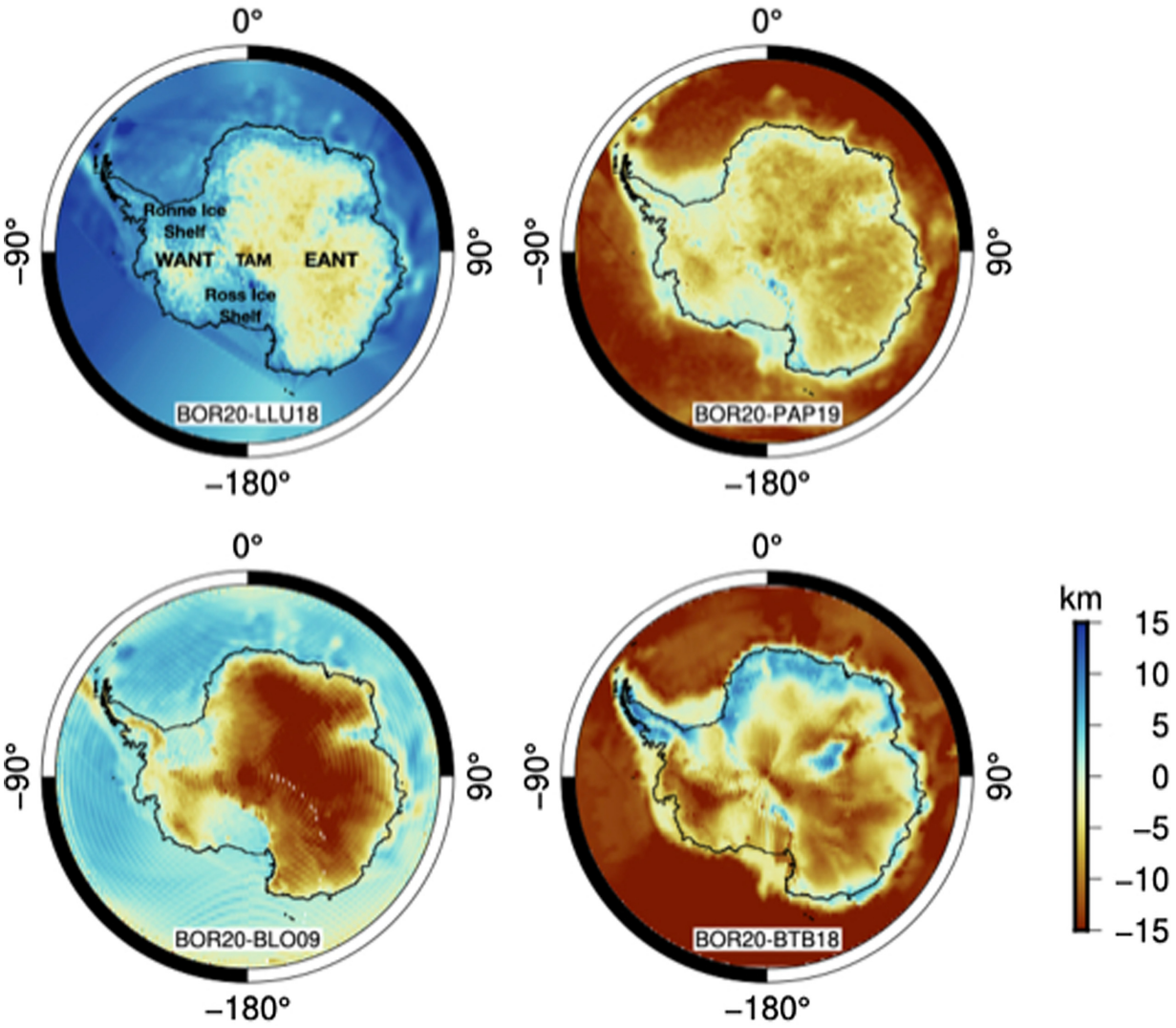

Figure 8. On the upper left, differences between the proposed model BOR20 and the LLU18 Moho (the Moho depth values are negative); on the upper right, differences between the proposed model and the PAP19 Moho; on the bottom left, differences between the proposed model and the BLO09; on the bottom right, differences between the proposed model and the BTB18. The values are in [km].

Table 4. Statistics of the differences in the Moho depths between the 206 values provided by An *et al* (2015) and the different models. Values in [km], where negative values mean deeper Moho of AN15 with respect to the considered model.

Model	Average	*SD*	Min	Max	RMS
BAR13	0.3	4.9	–13.2	17.0	4.9
PAP19	1.4	8.0	–19.0	16.7	8.1
LLU18	8.0	8.3	–12.6	27.9	11.5
BOR20	3.5	7.3	–12.2	20.4	8.1
BLO09	0.9	8.3	–21.2	21.6	8.4
BTB18	0.2	5.4	–26.5	16.1	5.4

First at all the comparison has been performed on single depth values reported in An *et al*. (2015). In Table 4 are reported the statistics of the comparison with the 206 depth values provided by An *et al*. (2015). The seismic model BAR13 shows a better agreement with these single depth values and among the gravimetric solutions PAP19 presents better statistical values. However, the standard deviations of the differences between the seismic values and the BOR20 model is lower with respect to the other gravimetric models.

In order to deeply investigate the behaviour of the different models, the Moho depths are compared along profiles that cross the whole Antarctica Region (Fig. 9).

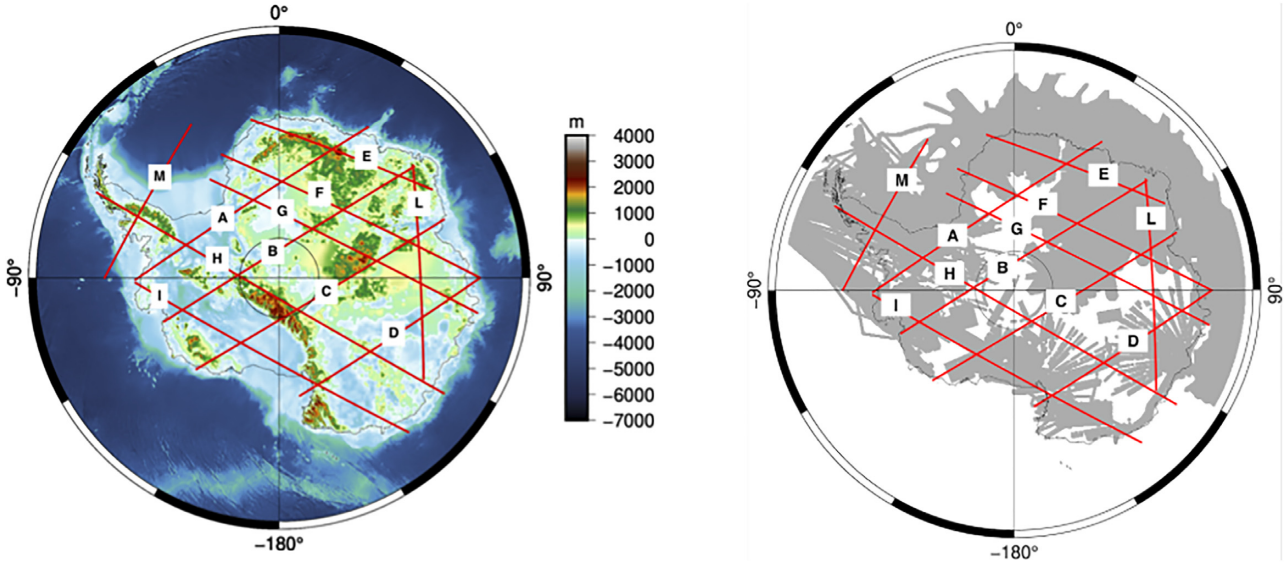

Figure 9. Distribution of the profiles along which the comparison between models have been performed with respect to the elevation map of Antarctica (on the left-hand side) and to the gravity data distribution of the ANTGG2015 database (on the right-hand side).

The first profile worth considering is profile A, because it goes through the thick sediment basin of the Ronne Ice Shelf and allows us to evaluate the effect of these sedimentary layers in calculating the depths of the Moho. When the gravity data are corrected for the three sediment layers presented in Baranov *et al*. (2018) (Fig. 10), the Moho surface in the Ronne Ice Shelf is deeper of about 2–5 km with respect to the solution without any sedimentary correction (Fig. 11. These differences, that could appear relevant, are also shown with respect to the other Moho solutions and the two new gravimetric estimates (with and without sediment correction) are both in the range of variability of the models. In the first part of the profile (from –70° to –45° of longitude) the solution corrected for sediment (cyan dashed line in Fig. 11) is very close to the original solution, however, for higher longitude, the discrepancies increase and the corrected estimate present a less smoother profile, that could suggest problem in this type of modelling.

In light of these considerations it is believed that further investigations are needed to test different sediment models and to reduce some border effects, visible in the reduced gravity values (Fig. 11). The next discussions will take into account only the BOR20 solution, that can be considered as a preliminary model, important for quantifying the strength of a pure gravimetric inversion for Moho definition, reducing eventually misfit due to the use of approximate models for densities and depths.

Analysing the profiles crossing the continent from west (WANT) to east (EANT, Fig. 12) it is possible to understand that the seven models taken into account (Table 4) are in agreement with each other in range of depths of more or less 10 km along the profile A and B, but this range increases for the other two profiles, C and D, that go through Marie Byrd Land and the Wilkes Basin respectively (Figs 9 and 12). Along the profile C the depth differences between WANT and EANT are more pronounced for the seismic models AN15 and BAR13, represented with red lines and that reach Moho depth differences of 10 km between east and west. The geodetic models along this profile are smoother except for the BLO09 solution that has a trend more similar to the ones of the seismic solutions, although it is shifted in depth. Similar considerations can be done for profile D although the AN15 shows a really shaped profile across the TAM region at longitude 160° (Fig. 12). The depths of BTB18 are more corrugated with respect to the other models, especially in the west part of profiles B and C. Focusing on the new gravimetric Moho BOR20, along these four profiles (A, B, C and D) BOR20 is deeper in the EANT with respect to the other models, however the trends of the BOR20 profiles are quite similar to the ones derived by BAR13, although the absolute values of the depths differs also for 10 km (i.e. profiles C and D).

Profile I (Fig. 13) is developed quite entirely in WANT and shows seismic Moho models (AN15 and BAR13) and BTB18 shallower than the other geodetic ones at west of the TAM (around longitude 160°): the seismic depths are in the range –20/–30 km, whereas the geodetic depths are in the interval –30/–40 km. In the short part of the EANT crossed by this profile, between longitude 160° and 140°, both types of models present a major agreement, converging in a narrower range of depths.

Profile M crosses the narrow Antarctica Peninsula and the Moho depths along this profile reflect the passage across the sea (Fig. 14). PAP19 and AN15 depths are very shallow in the oceanic part of the profile, but under the continental area of the Peninsula there is a fairly good agreement between models, in a range of values of less than 10 km. BOR20 and LLU18 present similar behaviour, but they are shifted each other, with LLU18 deeper than BOR20 and the other models.

Profile L crosses the EANT from north to south with respect to the representation of Fig. 9 and presents a very smooth Moho surface (Fig. 15). Under Amery Ice Shelf (around longitude 70°E) the Moho quickly rises, especially in the seismic models and in BOR20 and PAP19, rather than in BLO09 and LLU18 profiles where a more gentle slope is present.

The last set of profiles, E, F, G and H, crosses the EANT stopping along the TAM (Figs 9 and 16). Along profiles F and G the BOR20 Moho is on average deeper than the other solutions, but these two profiles go through regions where the ANTGG2015 database presents data

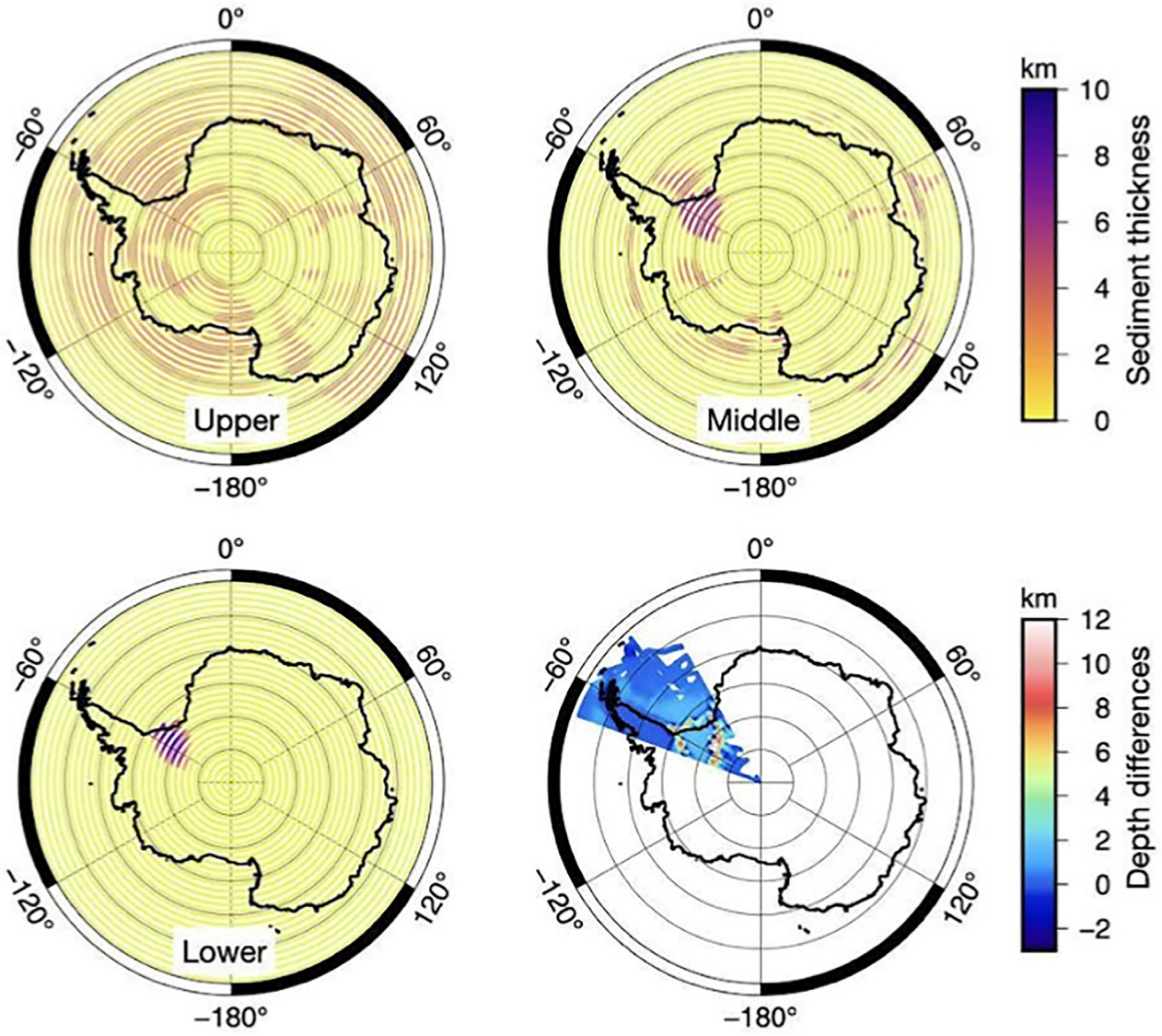

Figure 10. Upper, middle and lower layers of the sediment basins according to Baranov *et al* (2018).

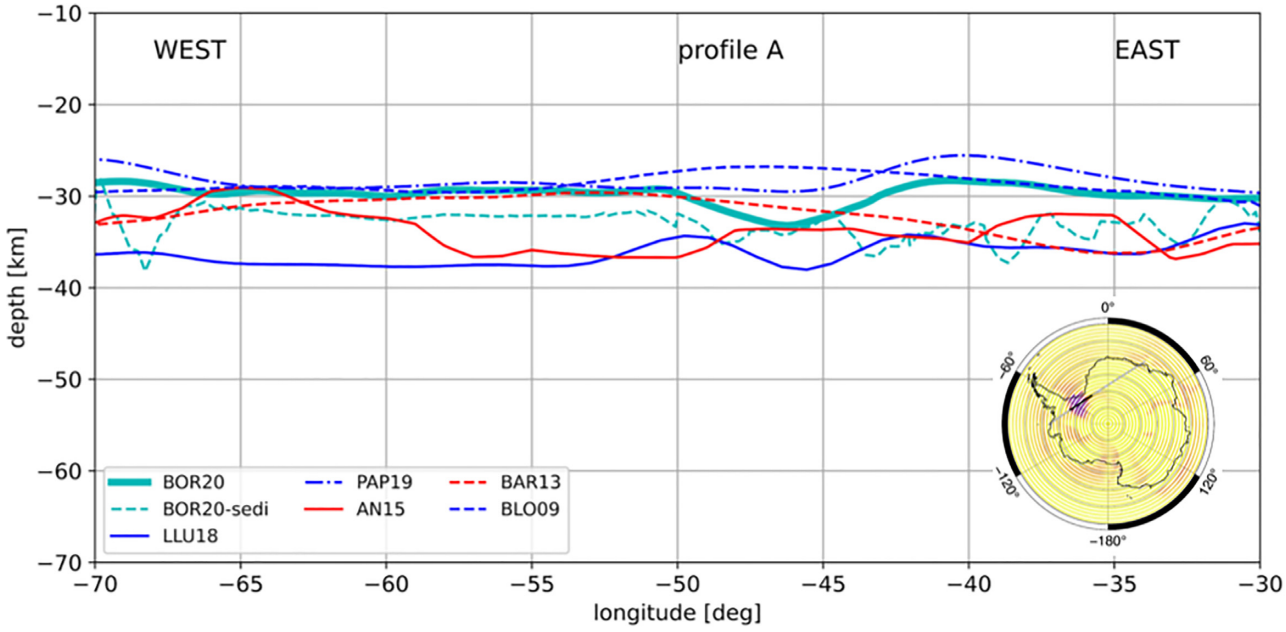

Figure 11. Moho depths along a segment of profile A between longitude –70°/–30°. The segment is the black line in the geographical image where the colours represent the total thickness to the three sedimentary layers of Baranov *et al* (2018).

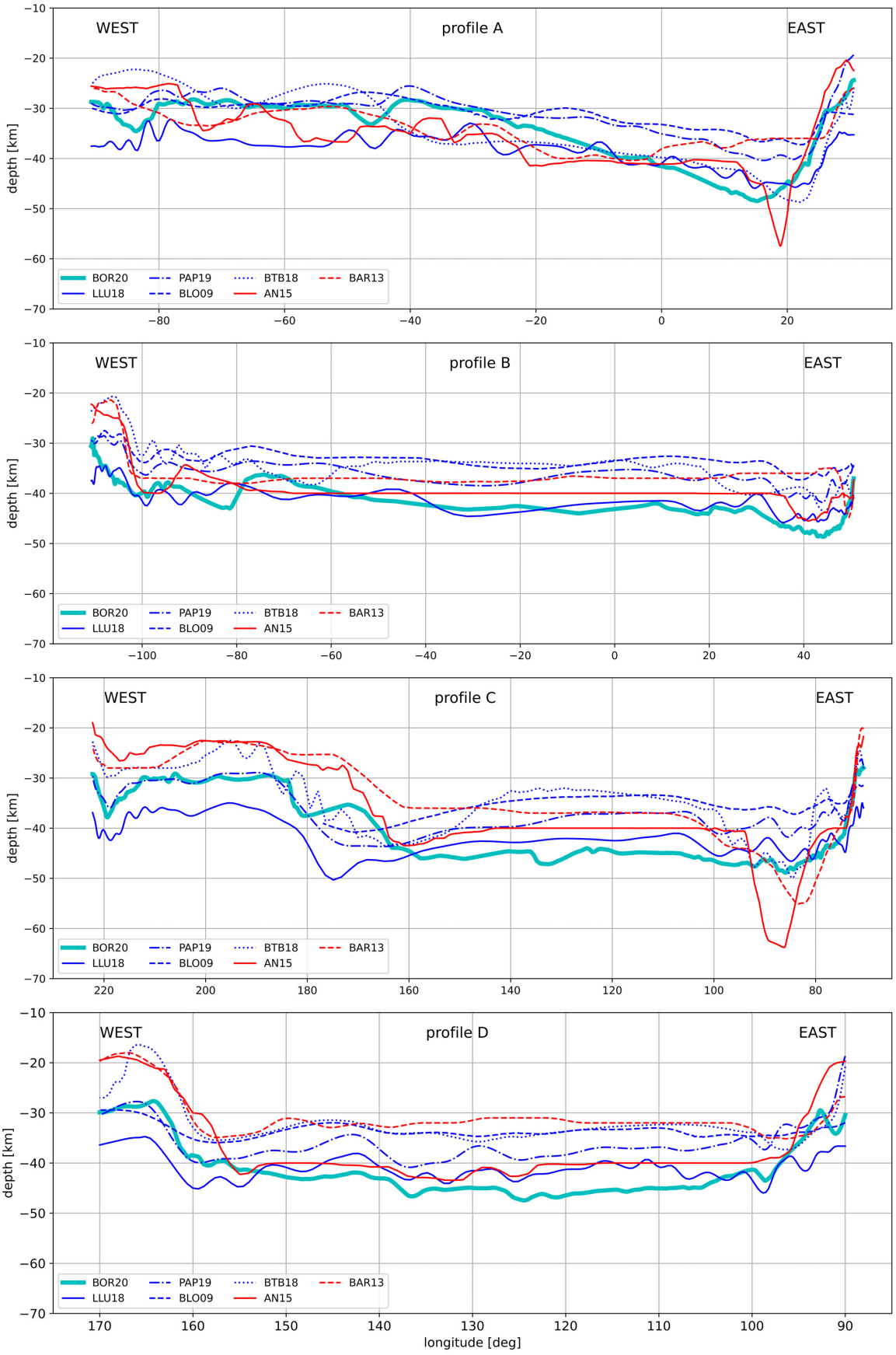

Figure 12. The four profiles that cross the Antarctica Region from west to east are reported from north to south with respect to the representation of Fig. 9.

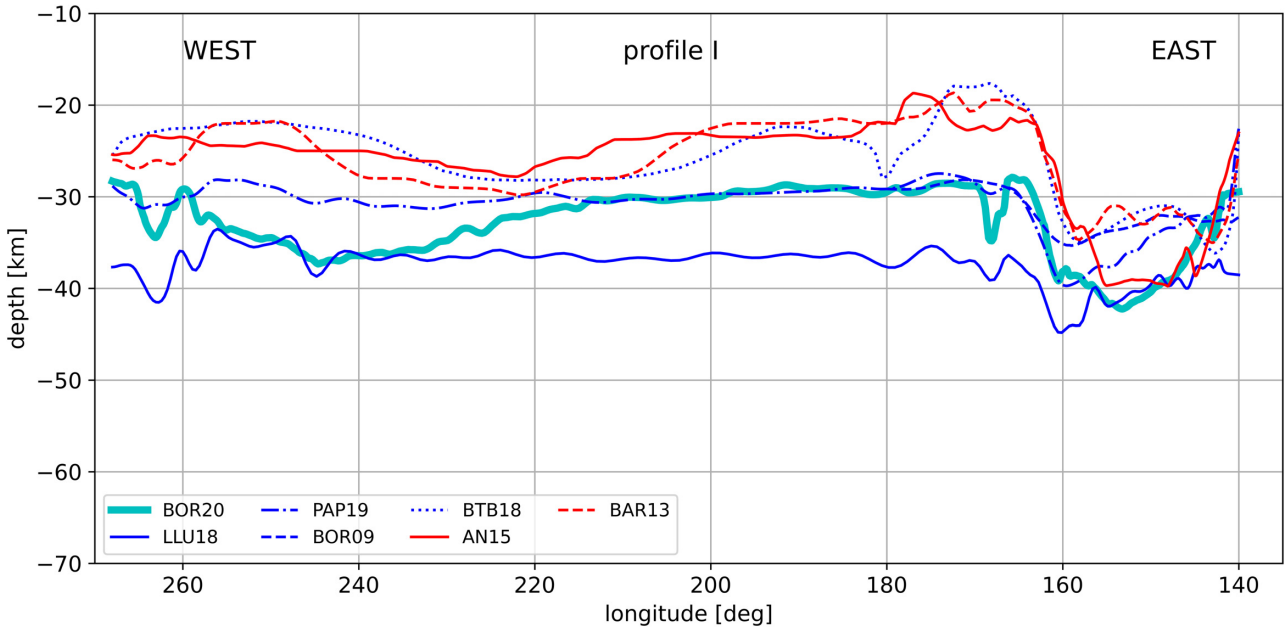

Figure 13. Profiles I in the WANT. The red lines represent the seismic models, whereas the blue ones are derived by gravity measurements.

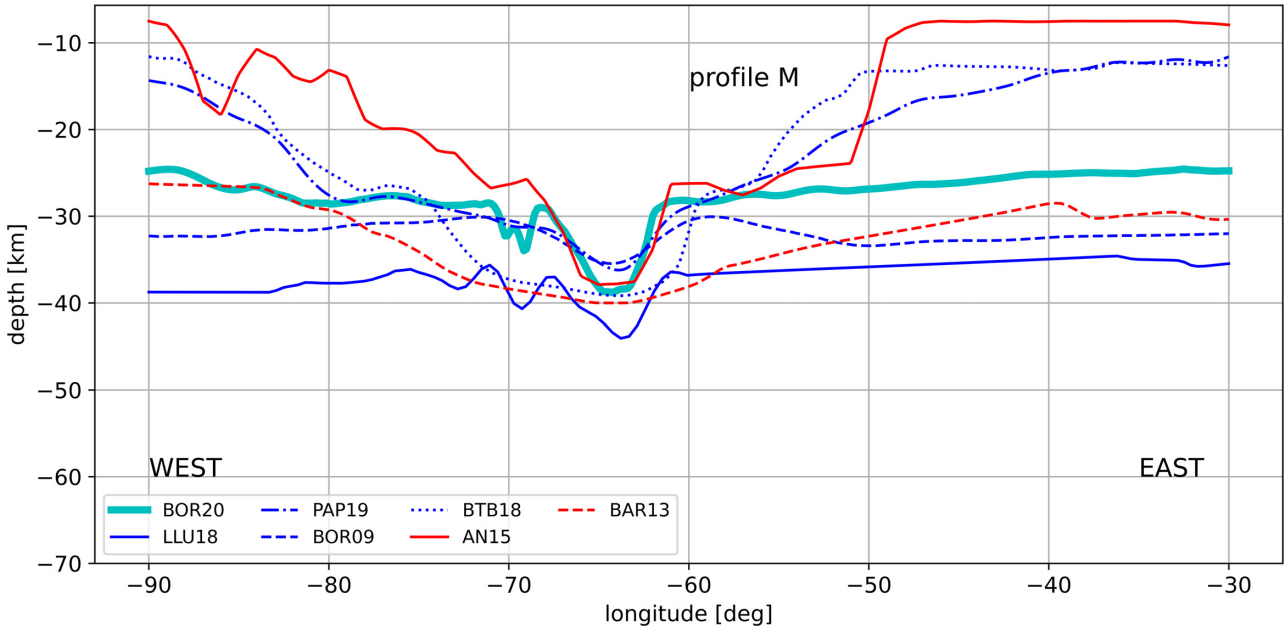

Figure 14. Behaviour of the profile M that crosses the Antarctica Peninsula.

gaps (Figs 1 and 9). Although the two models seem shifted between each other, the good agreement between BOR20 and LLU18 in terms of trend along the profile F suggests that the data gaps do not warp the Moho surface predicted by the inversion of the ANTGG2015 gravity data. Along profile H BOR20 and LLU18 depths are almost overlapping and this is an important result because the two Moho models used independent gravity data and different inversion methods, in fact LLU18 inverted the gravity values predicted by GO_CONS_GCF_2_DIR_R5 (Bruinsma *et al*. 2013), that is a global gravity field model obtained by satellite-only measures (GOCE, GRACE and altimeter missions), without introducing any ground-based gravity data.

The Moho models BOR20, PAP19, BLO09 and AN15 have been recently used in (Tondi *et al*. submitted) to reconstruct the upper mantle density and the related 3-D distribution of the couplings between density and seismic wave velocities up to 400 km of depth under the Antarctica Continent using the Sequential Integrated Inversion procedure (Tondi *et al*. 2012). In this context the impact of the Moho structure on the reconstruction of the mantle heterogeneities have been evaluated, selecting the before listed models. This work confirms that the major differences in the Moho depths in the EANT are reflected in the discrepancies among the intensities of the density anomalies and the density/seismic wave velocity couplings.

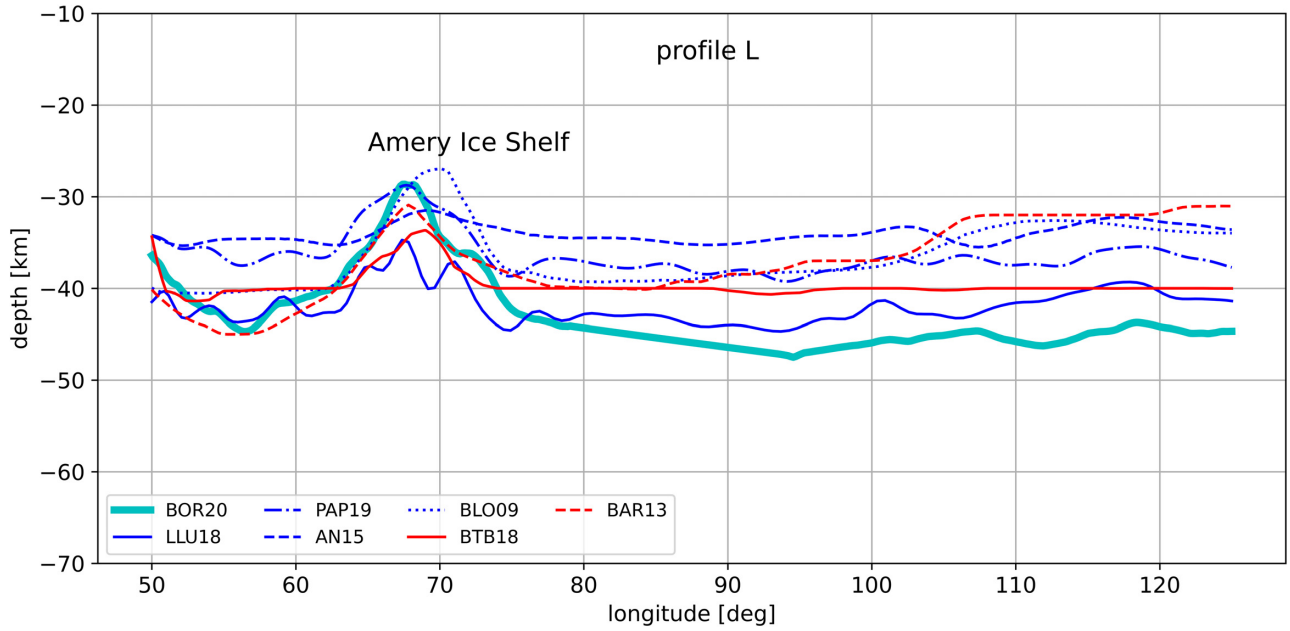

Figure 15. Moho depths along profiles L in EANT.

4 CONCLUSION

The BOR20 model for the Moho depths of the Antarctica Region has been obtained by the inversion of the ground-based gravity database ANTGG2015, whereas the other geodetic models were obtained by the inversion of the gravity data provided by global gravity field models, often mainly based on satellite gravity missions. Furthermore in the BOR20 solution no seismic and geological constraints have been introduced, so BOR20 can be considered as a pure gravimetric solution. In view of these considerations, the new estimate of the Antarctica Moho allows to investigate the potentialities of the inversion of ground-base gravity data for Moho definition and it represents also for the already available models a further and independent solution for cross-validating the knowledge of the Moho depths in this remote region of the Earth

The main results are summarized as follow:

(i) The new model BOR20 is less smooth than the other Moho models based on gravity observations, that have been taken into account in this work and that are characterized by a range of variability of the Moho depths of about 10–15 km. The BOR20 model based on ground gravity data is deeper in East Antarctica, reaching 50 km of depth, whereas in West Antarctica is shallower in the ice shelves, as Ross and Ronne ice Shelf, with about 30 km of depth.

(ii) Although the BOR20 model for the Antarctica Moho was obtained by a pure inversion of the ground gravity data using the LSC approach and without introducing external geological or seismic constraints, the obtained results are comparable in terms of trends and values to the other Moho models. This result proves the capability and the potentialities of the used approach and the reliability of the gravity database ANTGG2015.

(iii) This work can be considered a preliminary step toward an integrated approach for the definition of the depths of the Antarctica Moho, where different types of observations can be used to provide a unique solution. The integrated solution can be performed using, for instance, the LSC approach that requires the definition of the auto- and cross-covariance functions. In view of this integrated solution, it is important to know the accuracy and the correlation among the independent data and this work can be used to understand this aspect and tightly constraint in the next computation some more confident Moho depths.

ACKNOWLEDGMENTS

The author would like to thank the Italian National Antarctic program (Programma Nazionale di Ricerche in Antartide), because the idea of the presented work was born in the context of the project PNRA 2013/B2.06, the Editor and Reviewers for their contributions that helped improve this work. This work has been supported by the project INGV Pianeta Dinamico 2021-2022 Tema 4 KINDLE (grant no. CUP D53J19000170001) funded by the Italian Ministry of University and Research “Fondo finalizzato al rilancio degli investimenti delle amministrazioni centrali dello Stato e allo sviluppo del Paese, legge 145/2018”

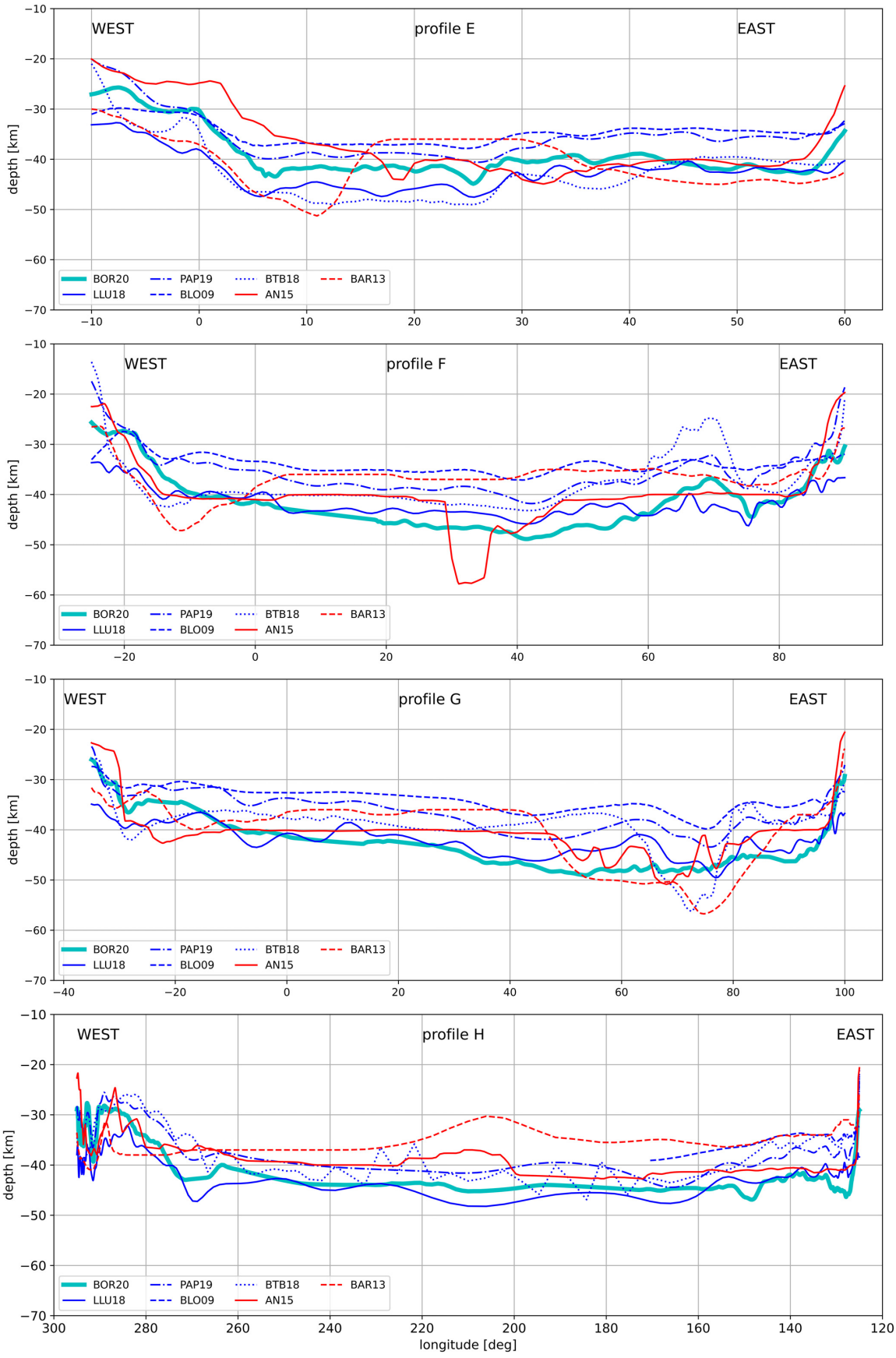

Figure 16. Profiles in the EANT up to TAM. The red lines represent the seismic models, whereas the blue ones are derived by gravity measurements.

DATA AVAILABILITY

The gravity database ANTGG2015 underlying this paper are available in PANGAEA Repository, at http://dx.doi.org/10.1594/PANGAEA.848168. The Earth2014 Rock Equivalence Topography (RET) is available at http://ddfe.curtin.edu.au/models/Earth2014/ (last accessed November 2021).

The Moho model BOR20 will be available at the INGV data set repository https://data.ingv.it and at https://zenodo.org/record/6811567#.YshG6S8QO-o.

REFERENCES

An, M. *et al.*, 2015. S-velocity model and inferred Moho topography beneath the Antarctic Plate from Rayleigh waves, *J. geophys. Res.,* **120,** 359–383.

Bagherbandi, M., Tenzer, R., Sjöberg, L.E. & Novak, P., 2013. Improved global crustal thickness modeling based on the VMM isostatic model and non-isostatic gravity correction, *J. Geodyn.,* **66,** 25–37.

Bagherbandi, M., Sjöberg, L.E., Tenzer, R. & Abrehdary, M., 2015. A new Fennoscandian crustal thickness model based on CRUST1.0 and a gravimetric–isostatic approach, *Earth-Sci. Rev.,* **145**(2015), 132–145.

Baranov, A. & Morelli, A., 2013. The Moho depth map for the Antarctica region, *Tectonophysics,* **609,** 299–313.

Baranov, A., Tenzer, R. & Bagherbandi, M., 2018. Combined gravimetric–seismic crustal model, *Surv. Geophys.,* **39,** 23–56.

Baranov, A., Morelli, A. & Chuvaev, A., 2021a. ANTASed – an updated sediment model for Antarctica, *Front. Earth Sci.,* **9,** doi:10.3389/feart.2021.722699.

Baranov, A., Tenzer, R. & Morelli, A., 2021b. Updated Antarctic crustal model, *Gondwana Res.,* **89,** 1–18, doi: 10.1016/j.gr.2020.08.010.

Barzaghi, A., Gandino, A., Sanso, F. & Zenucchini, C., 1992. The collocation approach to the inversion of gravity data, *Geophys. Prospect.,* **40,** 429–451.

Barzaghi, R. & Biagi, L., 2014. The collocation approach to Moho estimate, *Ann. Geophys.,* **57**(1), S0190, doi:10.4401/ag-6367.

Barzaghi, R., Reguzzoni, M., Borghi, A., De Gaetani, C., Sampietro, D. & Marotta, A.M., 2015. Global to local moho estimate based on GOCE geopotential model and local gravity data, in *Proceedings of the VIII Hotine-Marussi Symposium on Mathematical Geodesy. International Association of Geodesy Symposia,* Vol. **142,** eds Sneeuw, N., Novák, P., Crespi, M. & Sansò, F., Springer.

Bassin, C., Laske, G. & Masters, G., 2000. The current limits of resolution for surface wave tomography in North America, EOS, *EOS, Trans. Am. geophys. Un.,* **81,** S12A–03.

Block, A.E., Robin, E. & Studinger, M., 2009. Antarctic crustal thickness from satellite gravity: implications for the Transantarctic and Gamburtsev Subglacial Mountains, *Earth planet. Sci. Lett.,* **288,** 194–203.

Bott, M.H.P., 1960. The use of rapid digital computing methods for direct gravity interpretation of sedimentary basins, *Geophys. J. Int.,* **3**(1), 63–67

Bruinsma, S.L., Förste, C., Abrikosov, O., Marty, J.C., Rio, M.H., Mulet, S. & Bonvalot, S., 2013. The new ESA satellite-only gravity field model via the direct approach, *Geophys. Res. Lett.,* **40**(14), 3607–3612.

Capponi, M., Sampietro., D., Ebbing, J. & Ferraccioli, F., 2022. Antarctica 3-D crustal structure investigation by means of the Bayesian gravity inversion: the Wilkes Land case study, *Geophys. J. Int.,* **229**(3), 2147–2161.

Chen, W. & Tenzer, R., 2020. Reformulation of Parker-Oldenburg's method for Earth's spherical approximation, *Geophys. J. Int.,* **222**(2), 1046–1073.

Chisenga, C., Yan, J. & Yan, P., 2019. A crustal thickness model of Antarctica calculated in spherical approximation from satellite gravimetric data, *Geophys. J. Int.,* **218,** 388–400.

Ebadi, S., Barzaghi, R., Safari, A. & Bahroudi, A., 2019. Evaluation of different gravimetric methods to Moho recovery in Iran, *Ann. Geophys.,* **62**(5), doi:10.4401/ag-8054.

Eshagh, M., Bagherbandi, M. & Sjöberg, L., 2011. A combined global Moho model based on seismic and gravimetric data, *Acta Geod. Geophys. Hungar.,* **46**(1), 25–38.

Förste, C. *et al.*, 2014. EIGEN-6C4 The latest combined global gravity field model including GOCE data up to degree and order 2190 of GFZ Potsdam and GRGS Toulouse, GFZ Data Services., doi:10.5880/icgem.2015.1Abstr.

Fretwell, P. *et al.*, 2013. Bedmap2: improved ice bed, surface and thickness datasets for Antarctica, *Cryosphere,* **7,** 375–393.

David Gómez-Ortiz, D., Bhrigu, N.P. & Agarwal, B.N.P., 2005. 3DINVER.M: a MATLAB program to invert the gravity anomaly over a 3D horizontal density interface by Parker–Oldenburg's algorithm, *Comp. Geosci.,* **31**(4), 513–520.

Hirt, C. & Rexer, M., 2015. Earth2014: 1 arc-min shape, topography, bedrock and ice-sheet models – available as gridded data and degree-10,800 spherical harmonics, *Int. J. Appl. Earth Observ. Geoinform.,* **39,** 103–112.

Hofmann-Wellenhof, B. & Moritz, H., 2006. *Physical Geodesy,* Springer.

Krarup, T., 1969. A contribution to the mathematical foundation of physical geodesy, in *Mathematical Foundation of Geodesy,* Vol. **44,** pp. 29–90, ed. Borre, K., Springer.

Laske, G., Masters, G., Ma, Z. & Paysanos, M., 2013), Update on CRUST1.0 – a 1 degree global model of Earth's crust, *Geophys. Res. Abs.,* **15,** EGU2013–2658.

Laske, G. & Masters, G., 1997. A global digital map of sediment thickness, *EOS, Trans. Am. geophys. Un.,* **78,** F483.

Llubes, M., Seoane, L., Bruinsma, S. & Rémy, F., 2018. Crustal thickness of Antarctica estimated using data from gravimetric satellites, *Solid Earth,* **9,** 457–467.

Mayer-Gürr, T. *et al.*, 2015. The Combined Satellite Gravity Field Model GOCO05s, Vienna, Austria.

Moritz, H., 1990. *The Figure of the Earth,* Wichmann, pp. 353.

Oldenburg, D.W., 1974. The inversion and interpretation of gravity anomalies, *Geophysics,* **39,** 526–536.

Pappa, F., Ebbing, J. & Ferraccioli, F., 2019. Moho depths of Antarctica: comparison of seismic, gravity, and isostatic results, *Geochem., Geophys., Geosyst.,* **20,** 1629–1645, doi:

Parker, R., 1973. The rapid calculation of potential anomalies, *Geophys. J. R. astr. Soc.,* **31,** 447–455.

Pavlis, N.K., Holmes, S.A., Kenyon, S.C. & Factor, J.K., 2012. The development and evaluation of the Earth Gravitational Model 2008 (EGM2008), *J. geophys. Res.,* **117**(B4), doi:10.1029/2011JB008916.

Reguzzoni, M., Sampietro, D. & Sansò, F., 2013. Global Moho from the combination of the CRUST2.0 model and GOCE data, *Geophys. J. Int.,* **195**(1), 222–237.

Reguzzoni, M. & Sampietro, D., 2015. GEMMA: An Earth crustal model based on GOCE satellite data, *Int. J. Appl. Earth Observ. Geoinform.,* **35**(Part A), 31–43.

Reguzzoni, M., Sampietro, D. & Rossi, L., 2020. The gravimetric contribution to the Moho estimation in the presence of vertical density variations, *Rend. Fis. Acc. Lincei,* **31,** 69–81, doi:

Rossi, L., Reguzzoni, M., Sampietro, D. & Sansò, F., 2015. Integrating geological prior information into the inverse gravimetric problem: the Bayesian approach, in *VIII Hotine-Marussi Symposium on Mathematical Geodesy. International Association of Geodesy Symposia,* Vol. **142,** eds Sneeuw, N., Novák, P., Crespi, M. & Sansò, F., Springer.

Scheinert, M. *et al.*, 2016. New Antarctic gravity anomaly grid for enhanced geodetic and geophysical studies in Antarctica, *Geophys. Res. Lett.,* **43,** 600–610, doi:.

Shin, Y.H., Xu, H., Braitenberg, C., Fang, J. & Wang, Y., 2007. Moho undulations beneath Tibet from GRACE-integrated gravity data, *Geophys. J. Int.,* **170,** 971–985, doi:

Szwillus, W., Ebbing, J. & Holzrichter, N., 2016. Importance of far-field topographic and isostatic corrections for regional density modelling, *Geophys. J. Int.,* **207**(1), 274–287.

Tapley, B.D., Ries, J., Bettadpur, S., Chambers, D., Cheng, M., Condi, F. & Poole, S., 2007. The GFM03 mean Earth gravity model from GRACE,

EOS, Trans. Am. geophys. Un., **88**(52), Fall Meet. Suppl., Abstract G42A–03.

Tenzer, R., Hamayun, K. & Vajda, P., 2009. Global maps of the CRUST 2.0 crustal components stripped gravity disturbances. *J. geophys. Res.,* **114**(B5),.

Tenzer, R. *et al.*, 2015. Analysis of the refined CRUST1.0 crustal model and its gravity field, *Surv. Geophys*., **36,** 139–165.

Tikhonov, A.N. & Arsenin, V.Y., 1977. *Solutions of Ill-Posed Problems, Scripta Series in Mathematic,* Wimston.

Tondi, R., Cavazzoni, C. & Morelli, A., 2012. Parallel "large", dense matrix problems: application to 3D joint inversion of seismological and gravity data, *Comput. And Geosciences,* **48,** 143–156.

Tondi, R., Borghi, A. & Morelli, A. submitted, 3D density structure of upper mantle beneath the Antarctic plate: the influence of Moho structure.

Tscherning, C., 1985. Local approximation of the gravity potential by least squares collocation, in *Proceedings of the the Int. Summer School on local gravity field determination,* Beijing, China, Univ. of Calgary, Calgary Canada, Vol. 60003, pp. 277–362.

Uieda, L. & Barbosa, V.C.F., 2017. Fast nonlinear gravity inversion in spherical coordinates with application to the South American Moho, *Geophys. J. Int.,* **208,** 162–176.

Vening Meinesz, F.A., 1931. Une nouvelle méthode pour la réduction isostatique régionale de l'intensité de la pesanteur, *Bull. géodésique,* **29,** 33–51.

Wiens, D.A., Shen, W. & Lloyd, A.J., 2021. The seismic structure of the Antarctic upper mantle, in *The Geochemistry and Geophysics of the Antarctic Mantle,* Vol. 56, Memoirs, eds Martin, A. P. & van der Wal, W., Geological Society London.